Inter*net* Electronic Journal*

Nanociencia et Moletrónica

Junio 2013, Vol.11, N°1, pp 2019-2030

Nanostructure PbS Thin Films

[1]Clemente Aguilar Galicia, [2]M. Zamora Totot zintle, [2]I. Galicia Morales [2]A. Camacho Camacho Yáñez, [2]L. Chaltal Lima, [2*]Oscar Portillo Moren

1. Preparatoria Regional Simón Bolívar, Atlixco Puebla, Pue. México de la Benemérita Universidad Autónoma de Puebla, CP7 2570, Puebla, México

2. Facultad de Ciencias Químicas, Benemérita Universidad Autónoma de Puebla (BUAP), México.C. U. Tel. (01 222) 2 29 55 00 Ext. 7519. Puebla, México, Puebla, México.

recibido: 18.11.12 revisado: 22.02.13 publicado: 31.07.13

Citation of the article;
Clemente Aguilar Galicia, M. Zamora Totot zintle, I. Galicia Morales A. Camacho Camacho Yáñez, L.Chaltal Lima, Oscar Portillo Moren, Nanostructure PbS Thin Filmss, Int. Electron J. Nanoc. Moletrón, 2013, Vol. 11, N°1, 2019-2030

Nanostructure PbS Thin Films

[1]Clemente Aguilar Galicia, [2]M. Zamora Tototzintle, [2]I. Galicia Morales [2]A. Camacho Camacho Yáñez, [2]L. Chaltal Lima, [2*]Oscar Portillo Moren

1. Preparatoria Regional Simón Bolívar, Atlixco Puebla, Pue. México de la Benemérita Universidad Autónoma de Puebla, CP7 2570, Puebla, México

2. Facultad de Ciencias Químicas, Benemérita Universidad Autónoma de Puebla (BUAP), México.C. U. Tel. (01 222) 2 29 55 00 Ext. 7519. Puebla, México, Puebla, México.

recibido: 18.11.12 revisado: 22.02.13 publicado: 31.07.13

Internet Electron. J. Nanoc. Moletrón., 2013, Vol.11 , N° 1pp 2019-2030

Abstract. Nanocrystalline PbS films were grown onto glass substrates by chemical bath deposition (CBD). The temperature of the bath (T_d) was selected in the interval: 80-0°C., Scanning Electron Microscopy, X-ray diffraction, optical absorption, measurements were carried out to characterize the films. Using the SEM, we analyzed the morphological changes. Spectra of DRX show peaks the angular positions: 2θ = (26.00, 30.07, 43.10, 51.00, 53.48), growth on zinc blende face. Average grain size (GS) decrease monotonically ~32-20 nm. Tthe optical band gap forbidden (E_g) shift 1.92-2.3 eV range.

***Keywords*:** Thin films, nanocrystals, potential cell, quantum confinement, coordination complex

Resumen. Películas nanocristalinas de PbS**,** fueron crecidas sobre sustratos de vidrio mediante la técnica de Deposito por Baño Químico (DBQ). La temperatura de baño (Td) fue seleccionada en el intervalo 0-80°C. Mediante Microscopia electrónica de barrido, Difracción de Rayos X y Absorción Óptica, fueron utilizadas para caracterizar las películas..Utilizando MEB los cambios morfológicos son analizados. Los espectros de DRX muestran picos en las posiciones angulares: 2θ = [26.00, 30.07, 43.10, 51.00, 53.48], con crecimiento en fase cubica o zinblenda. El tamaño de grano (TG) disminuye monoticamente de ~32-15 nm. De la Transmitancia se calcula el corrimiento del ancho de energía prohibida (E_g) en el intervalo 1.92-2.35 eV. Palabras clave: Películas delgadas, nanocristales, potencial de celda,

1. Introduction

The increasing research in nanotechnology is producing a wealth of new materials for which much of the basic characterization is missing. There are many reasons for this lack of date about nanocrystals (NCs), for example, reported synthesis are often not sufficiently reproducible, or the resulting material does not have the quality or purity that is required for many in-detail studies. One of the consequences is that, more and more, advanced experiments are slowed by the unavailable of proper data regarding some basic properties of these NCs [1]. PbS NCs can be used in electroluminescent devices such as light-emitting diodes, and optical devices such as optical switches due to the high third-order nonlinear optical properties [2]. Semiconductor NCs display a wealth of size-dependent physical and chemical properties, including quantum confinement effect, shape dependent electronic structure, and control over assembly through modification of surface functionalization. Photovoltaic devices are easily recognized potential applications NCs due, in part, to their high photoactivity, solution processability and low cost of production. Several schemes for using NCs in solar cells are under active considerations [3]. The Pb chalcogenide family of NCs in actively investigated for NCs solar cell applications because they have such large exciton Bohr radii (PbS 18 nm), in the limit where the NCs are only a tenth or so the bulk exciton diameter, electrons and holes can be tunnel through a thin organic surface coating, and therefore strong electronic coupling between particles facilities transport of charge between NCs. Thin films of lead and cadmium sulphate are a promising photo voltaic materials as their variable forbidden band gap energy (E_g) could be adjusted to match the ideal E_g = 1.5 eV required for archiving a most efficient solar cell. The optical properties of these NCs are interest because their characteristics are related with the size with nanometer dimensions of 2-18nm. The PbS is a semiconductor with E_g = 0.41 eV, which has continuous absorption in a short wavelength. Physical and chemical methods have been reported about the method of obtaining NCs as polycrystalline films using several deposition techniques, one of the simplest being the chemical bath (CB) [4, 5, 6, 7, 8]. CB is of special interest as it a simple, but highly efficient method. It provides a powerful and versatile control of used for preparation of high quality PbS NCs growth films, has been investigated thoroughly for numerous substrates *e.g*. glasses, polymers, and semiconductors [8]. The aim of this work was to investigate NCs PbS growth by CB in temperature deposited (T_d) 80-0°C range. Surface morphology and composition were determined using Carl Zeiss Auriga 39-16 accompanied with a Bruker energy dispersive analysis of X-Rays (EDAX). The-ray diffraction (XRD) spectra were obtained utilizing a D8 Discover diffractometer, using the Cu K_α line. The optical absorption spectra, measured employing a Unicam 8700 Spectrometer, allowed us to calculate the E_g, by using the $(\alpha h\nu)^2$ vs $h\nu$ plot, where α is the optical absorption coefficient and $h\nu$ the photon energy.

2. Thermodynamic model and Experimental

The reactions for the growth of PbS films have been investigated by employing the cell potential values in basic media reported in the literature [9]. The cell potential and the Gibbs free energy are related through the Nernst equations: $\Delta G^0 = - n\tau\varepsilon^0$, where n is the number of equivalents, τ is the Faraday constants and ε^0 are the cell potential, ΔG^o is calculated in the stages of the reaction [5, 6].

$$SC(NH_2)_2 + 3OH^- \Leftrightarrow CO_3^{2-} + S^{2-} + 7H^+ \quad (1)$$

$$[Pb(NH_3)_4]^{2+} + 2e \Leftrightarrow Pb + 4NH_3 \qquad \Delta G^0 = +118.30\ KJ \quad (2)$$

$$HPbO_3^- + H_2O + 2e \Leftrightarrow Pb + 3OH^- \qquad \Delta G^0 = +104.20\ KJ \quad (3)$$

The reaction of semicelda of PbS for the formation of the ion S^{2-} and elementary Pb

$$PbS + 2e \Leftrightarrow Pb + S^{2-} \qquad \Delta G^0 = +179.40\ KJ \quad (4)$$

$$PbS + 2e + 2H^+ \Leftrightarrow Pb + H_2S \qquad \Delta G^0 = +177.66\ KJ \quad (5)$$

$$Pb(OH)_2 + [Pb(NH_3)_4]^{2+} + Pb + 2S^{2-} + 2H^+ \Leftrightarrow PbS + 4NH_3 + H_2S + 2OH^-$$

$$\Delta G^0 = -2.20\ KJ \quad (6)$$

Based on the Gibbs free energy values obtained from the thermodynamic equilibrium analysis, under our work conditions by comparing the changes in $\Delta G^0 < 0$,' is thermodynamically probable to growth PbS films. [12].

The substrates cleaning was carried out immersing them into and acid-chromium [$K_2Cr_2O_7$/HCl/H_2O] mixture for 24 h and then rinsing them in deionised water and dried in a clean hot–air flow. The polycrystalline PbS thin films were growth by chemical bath CB using deionised water solutions: $Pb(CH_3CO_3)_2$ (0.01 M), KOH (0.5 M), NH_4NO_3 (1.5 M), $SC(NH_2)_2$ (0.2 M). The solutions were mixed and the final solution heated at corresponding temperature of the bath (T_d) for 15 min-2 h, according T_d, with the substrates remaining inside solution [6]. All the solutions used were prepared with deionised water of resistivity 18.2 MΩ. The samples were labelled PbS0, PbS10,...., PbS80, were 0, 10,..., 80 are T_d. The films was, homogeneous, polycrystalline reflective and with good adhesion to the substrate. The aim of this work is to find the optimum conditions for growth PbS NCs thin films at different deposit temperature T_d to investigate structural, optical the PbS NCs films.

3.1 Scanning *Electron Spectroscopy* (*SEM*)

In order to examine the influence temperature and compare their effect on the PbS films were deposited at temperature (T_d) 0-80°C range. The Figure 1 show a typical EDAX pattern and details of relative analysis PbS films. The quantitative analysis of the films was carried out by using the EDAX technique. Table 1 are compiled atomic concentrations of Pb and S. The elemental analysis was carried: (*a*) Na, C, Si and O were the glass substrate, Pb and S for PbS films (*b*) Pb and S. In general, the average atomic percentage of Pb/S was stoichiometric films.

Pb, S concentrations in PbS samples values studied by means Scanning Microscopy Electron (SEM)

Deposit Temperature (ºC)	Pb	S
0	49.89	50.11
10	48.85	49.15
20	46.09	53.91
30	47.16	52.84
40	48.9	51.1
50	49.89	50.11
60	49.89	50.11
70	47.55	52.45
80	47.50	52.50

Table 1. Pb, S, concentrations in PbS layers; T_d = 80. 70, 60, 50, 40, 30, 20, 10, 0°C.

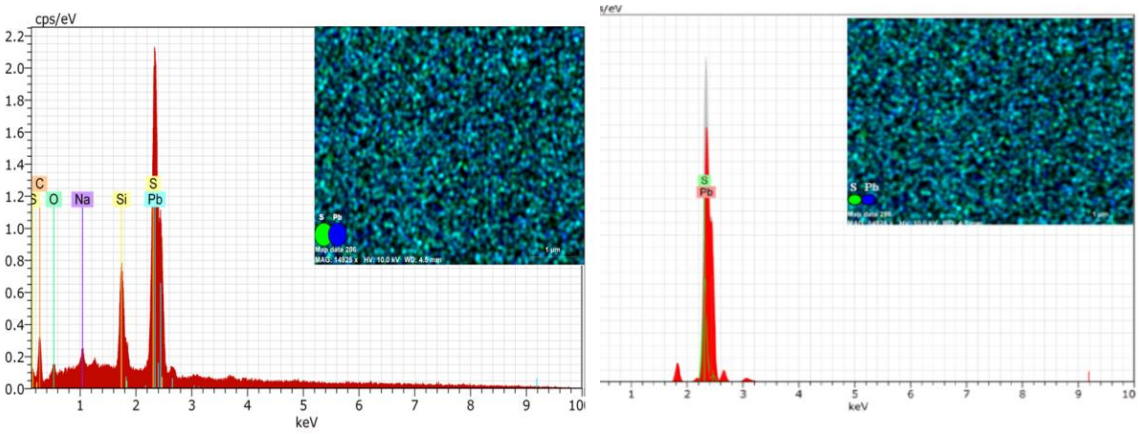

Figure 1. Typical EDAX patterns PbS thin films deposited on a glass substrate. The elemental analysis was carried (*a*) Na, C, Si and O was the substrate glass, Pb and S. (*b*) for PbS samples, Pb and S.

Figure 2. It can be is appreciated the SEM micrograph was obtained from Scanning Electron Spectroscopy (SEM) of PbS: T_d = 80, 50, 0°C. Very adherent films reveal existence of a continuous compact polycrystalline film. These films you can see the uniform surface morphology, which is compact and polycrystalline nature. The SEM micrographs show that the particle grain size decreases with decreases T_d. The granules are made of different sizes; we can conclude that T_d plays a vital role on the morphological properties of the NCs PbS thin films. The micrographs of the films PbS10, PbS20, PbS30, PbS40, PbS60, and PbS70 are not shown; the data sets were found nearly identical. These micrographs are appreciated for PbS50- and PbS0 films have crystals in the form of spheres small. A very adherent film with gray-black colour metallic aspect was obtained films reveals a continuous compact polycrystalline films. Similar morphology has been reported [14]. In Figure 2 you can see the uniform surface morphology compact and polycrystalline nature are homogeneous and they cover the glass substrates well. The SEM micrographs show that the particle grain size decreases with decrease T_d, and the granules are of different sizes.

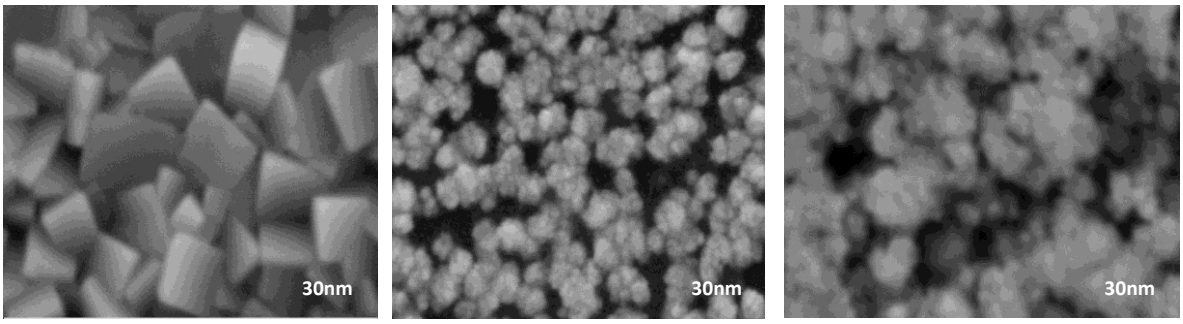

(a) (b) (c)

Figure 2. Micrographs of SEM with scale 30 nm for films: (a) PbS80, (b) PbSN50, (c) PbS0 films respectively.

3.2. X-*Ray Diffractions* (*XRD*)

Figure 3 shows sample diffractograms XRD PbS films 80-0°C. These spectra of x-ray show peaks located at the angular positions: 2θ = (26.00, 30.07, 43.10, 51.00, 53.48). are clearly distinguished, and all these diffraction peak can be perfectly indexed to diffractogram of the PbS samples display the Zinc blende (ZB) crystalline phase belong to the ZB phase according to reference patterns JCPDS 05-0592. The layer PbS10 diffraction along the [200] plane shows the highest intensity well-defined sharp peak, indicated high crystalline of the films. Sharp diffractions peaks for NCs, including nanopowders, nanowires, nanotubes, nanorods and nanosheet, have broadly been observed, which attributed to high crystallinity [7].The intensity of this peak reached a maximum value for the sample indicates either the existence of larger number of [200] planes or the [200] planes have a lower number defects. These effect is associated whit the regime were the cluster mechanism dominates (contrary to films grown via ion-ion mechanism, were the crystal size was much larger), consist of PbS NCs. Figure 4 show average grain size (GS) vs T_d calculated from the width of the main peak of the XRD patterns of PbS 80-0°C, in the (200) crystalline plane, the average grain size (GS) of PbS 34-20 nm, for the sample PbS10 film can be seen at a relative minimum of ~ 20 nm.

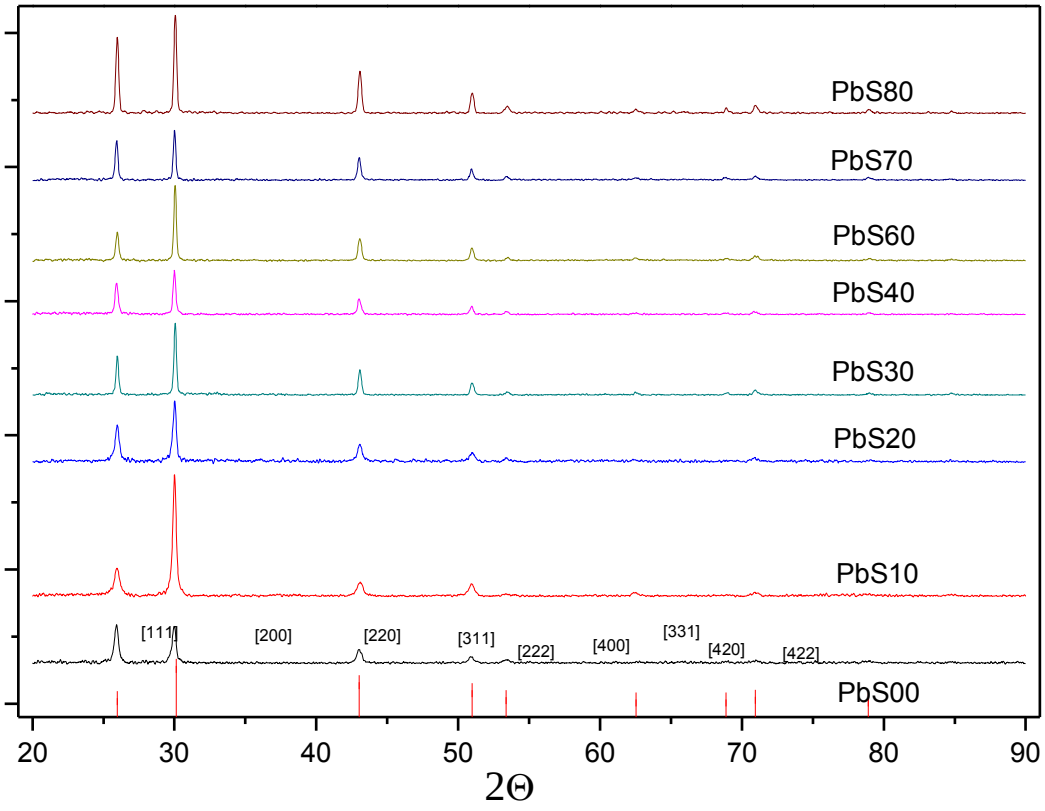

Figure 3. Diffractograms of X-ray (XRD) for films T_d = 80-0°C.

In this plot, it is possible to see that the GS decreases in oscillatory from to 80°-0°C and with significant change for PbS10 and PbS20 layers respectively. This phenomenon may be attributed to stability NCs PbS has effect on crystal growth. The lower T_d will favour the increment in the [200] plane growth rate. This process ocurr as result if decreased T_d. The T_d dependet effects are a result of change of GS due to law growth rate. The evolution of the film morphology is strongly affected by transition of the active deposition mechanism during the curse of the deposition. With decrease T_d, the contribution of the cluster mechanism is strongly decreases, resulting in a tendence to form larger crystal wich growth by ion-ion deposition mechanism. PbS10 and PbS20 the grain density reduced indicating the smaller grain of PbS the GS is noticed. The surface roughness is unavoidable since the grains are growth with different sizes. The surface roughness is very small (~10.5 nm). PbS10 and PbS20 layer shows that the small nanograins of ~20 nm size were uniformly distributed over the smooth homogeneous background crystalline phase.

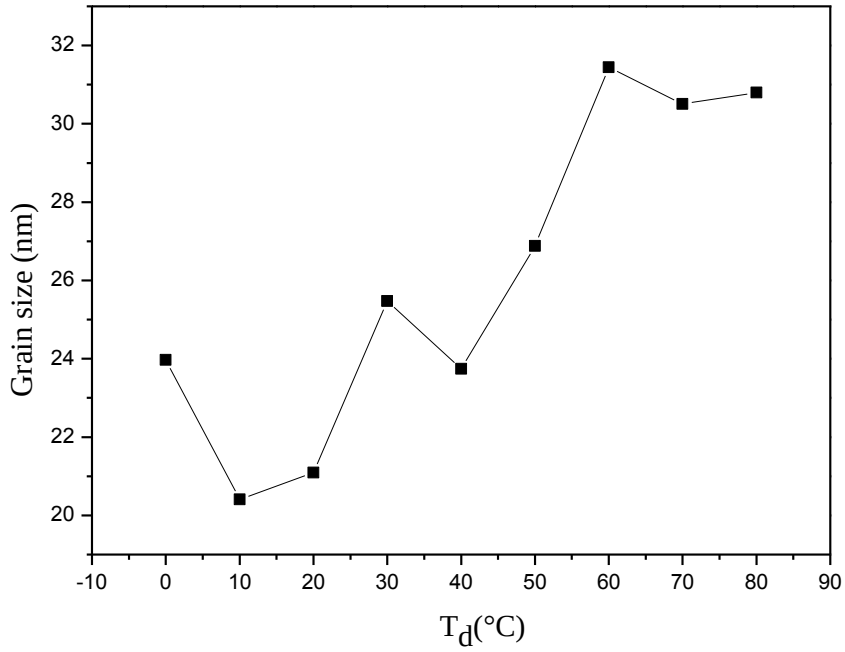

Figure 4. Average grain size (GS), PbS80- 0°C in the [200] crystalline plane.

3.6. *Optical Absorption* (*OA*)

The refractive index *n* and the thickness *d* of the layer were estimated from the reflection spectra. Assuming parabolic band structure, the absorption coefficient α is proportional to $(E-E_g)^{1/2} = \alpha h\nu$, were $h\nu$ ids photon energy Eg forbidden band gap, α absorption coefficient. An extrapolation to $\alpha^2 = 0$, yields a good approximation of the E_g [16]. PbS is a narrow gap semiconductor with extreme of conduction and valence band at the *L* point of the Briollouin zone. Energy gap direct $(E^{+}_{g,direct} - E^{-}_{g,direct})$: 0.41 eV, T = 300 K. The critical point energies are related to transitions *e.g*. Σ(4→7), which means a transition occurring along Σ-symmetric line between the 4th and 7th band. The bands are counted such a way that the uppermost valence band has number 5 and the lowest conduction band number 6. E_1 = 1.85 eV, T= 300 K, *E*(Σ*L*(5→7)) 1.98 eV, T = 297 K, E_2 = 3.49 eV, T = 297 K [18], *E*(Σ*L*(5→7)) 3.7 eV, T = 300 K, *E*(Δ*L*(5→6)) 4.0 eV, T = 300 K, *E*(Δ*L*(5→6)) 4.6 eV, T = 300 K, [17, 18]. The fundamental absorption (0.41 eV) which corresponds to electron excitation from the valence band to conduction band can be used to determine the nature and value of E_g. Through the intersection of the straight line with the axis of the photon energy is obtained E_g. Is obtained E_g in a similar way to the all samples. Figure shows 5 the spectra $(\alpha h\nu)^2$ vs. $h\nu$ in 1.5-3.0 eV range the optical fundamental absorption for the all samples.

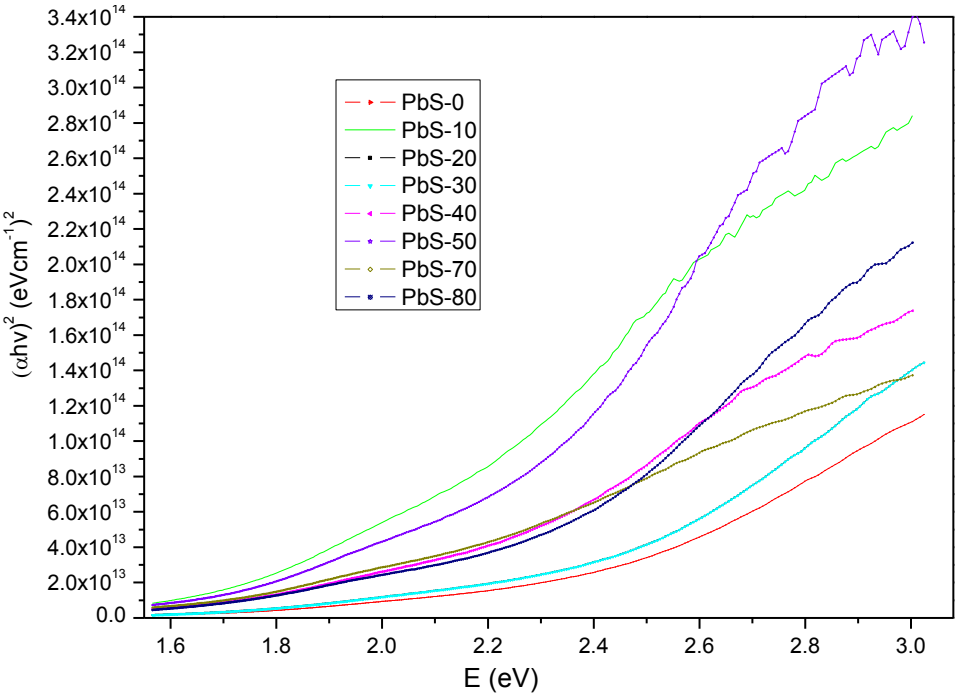

Figure 5. $(h\nu\alpha)^2$ versus $h\nu$ 1.5-3.0 eV range of PbS films.

In this plot. the curves in layers PbS80, PbS70, PbS60, PbS50, show a weak wide shoulder around 0.45 eV, associated with NCs with GS >20 nm. The Figure 6 shown E_g vs. T_d the PbS and the inset of the same plot show the spectrum of absorption for the sample. The inset illustrates the method to calculate E_g from optical absorption measurements [19]. While the remains spectra 1.9-2.3 eV are dominated by PbS NCs, this curves reveals that the optical band gap of NCs, showing a shift with respect to bulk PbS (0.4 eV) material, due to size quantization. Also reveals that of the various NCs samples is Stocks shifted from corresponding absorption edge ~0.6 eV. The Stocks shift indicate that the NCs is associated with electron-hole (deep-hole traps and shallow electron traps) could be associated with imperfections at the surface of the NCs, the passivation at the surface is not complete, leaving dangling bonds, excess to external adatoms or stoichiometric defects. Thus the trapped carriers can be distributed around the periphery of the NCs, with a statical mutual distance that does not exceed the diameter of the larger NCs. It is observed from the ratio that the quantization size effect increases on decreases the T_d in PbS films. It is seen that the size effect on the E_g optical is stronger for low T_d nanoparticle films. The observed increase in the quantum size effect could possibly be attributed to a decrease in effective mass and increase in binding energy over that in PbS NCs [20]. The proposed decrease in effective mass in the PbS films is also reflected in the observed increase in the experimentally measured in Hall mobility [21]. The confinement effect appears as a shift in absorption spectra and the absorption to lower wavelengths, wicks is due to change in the E_g. This is due the decrease in GS, the decrease in number of defects and the change in color. It is clearly seen from the

optical spectra that the absorption edge shifts toward a longer energy films. The shift experimentally observed E_g values by other authors [22, 23]. Figure 6 shown that the E_g vs.

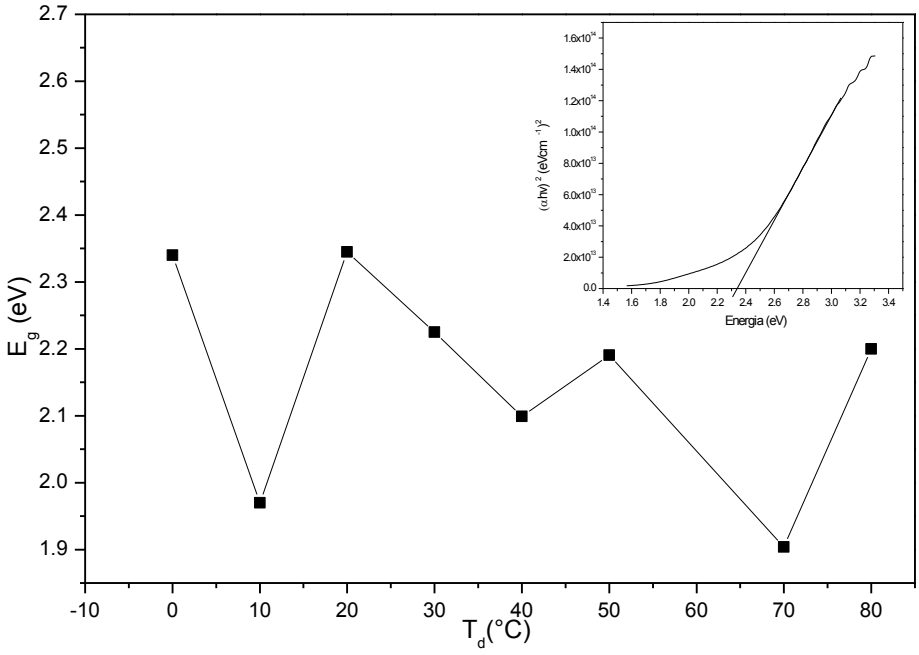

Figure 6. E_g as function of T_d. The inset illustrates the method to calculate E_g from optical absorption measurements.

T_d for all samples, the large experimentally observed E_g in the NCs films to theorically estimated (using Vega*r*'ds law) E_g for bulk shows the extent of quantum size effect in NCs films. It is seen that size effect on the E_g optical is stronger NCs films than in PbS NCs of 24-10 nm (average crystallite size) show a E_g: 2.22-2.65 eV [24]. The increased in E_g with decrease in T_d in the films is reflected by the presence of excitonic structure material. Excitonic structures are readily observed in large E_g semiconductors with binding energy such as CdSe [23]. The E_g optical films varied from ~1.95-2.5 eV, with increase T_d. A similar observed shift in the position of the excitonic peak towards higher energies in CdSe NCs has been explained as being due to decrease in crystallite size [23]. The shift of the E_g is associated with the decline of the SG, it is clear that the E_g increase when T_d decrease. Using already published data a NCs size of 4-5 nm corresponding to E_g = 1-1.25 eV, 3.8 nm for E_g = 1.4 eV, 2.7 nm for E_g = 2.0 eV and 2 nm for E_g = 2.7-3.8 eV respectively. The shift is attributed to quantum confinement of charge carriers in the NCs. One can see that the E_g of PbS can broaden easily with decreasing crystal due to relatively small m^* for PbS (compared with other semiconductors), which can bring about a large shifts on the absorption edge. No obvious absorption for the NCs with average size TG >20 nm, which is due to the crystal than exciton Bohr radio of PbS.

Acknowledgements

The authors thank to Maestro Rubén Romero Corona Director de la Preparatoria Regional Simón Bolívar de la Benemérita Universidad Autónoma de Puebla, AND M. C. G, Quiroz Oropeza Director de la Facultad de ciencias Químicas de la Benemérita Universidad Autónoma de Puebla, for the support given to the publication of this work.

Conclusions

The spectra of x-ray show peaks located at the angular positions: 2θ = [26.00, 30.07, 43.10, 51.00, 53.48]. The layer PbS10 diffraction along the [200] plane shows the highest intensity well-defined sharp peak, the GS films can be seen of ~20 nm. The spectra optical, it can be observed E_g ~1.95-2.5 eV, with increase T_d. A similar observed shift in the position of the excitonic peak towards higher energies in PbS NCs has been explained as being due to decrease in crystallite. The shift of the E_g is associated with the decline of the SG. The shift is attributed to quantum confinement of charge carriers in the NCs.

References

[1] Ludovico Cademartiri, Erica Montanari, Gianluca Calestany, Andrea Migliori, Antonietta Guagliardi, and Geoffrey A. Ozin, J. Am. Chem. Soc. **128** (2006) 10337-10346.
[2] R. S. Kane, R. E. Cohen, and R. Silvey, Chem. Mater, **8** (1996) 1919-1924.
[3] Jian Xu, Dehu Cui, Ting Zhu, Gary Paradee, Ziqi Liang, Qing Wang, Shengyoung and Andrew Y Wang, Nanotechnology **17** (2006) 5428-5434.
[4] Anna Osherov and Yuval Golan, phys. stat. sol. **5** (2008) 3431-3436.
[5] O. Portillo Moreno, M. Chávez Portillo, M. Moreno Flores, J. Martínez Juárez, G. Abarca Ávila, R. Lozada Morales, O. Zelaya Ángel, Journal of Materials Science and Engineering **A 1** (2011) 759-767.
[6] O. Portillo Moreno, G. Abarca Ávila, J. R. Cerna, J. Hernández Tecorralco, M. Chávez Portillo, J. Martinez Juárez, R. Lozada Morales, O. Zelaya Ángel, Journal of Materials Science and Engineering **B 1** (2011) 692-704.
[7] Huaquiang Cao, Gouozhi Wang, Sichun Zhang and Xinrong Zhang, Nanotechnology **17** (2006) 3280-3287.
[8] Alex P. Gaiduk, Peter I. Gaiduk, Arne Nylandsted Larsen, Thin Solid Films **516** (2008) 3791-3795.
[9] A. J. Bethune and N. A. S. Loud, *in Standard Aqueous Potential and Temperature Coefficients at 25°C*, C. C. Hampel, Skokie, II. (1969).
[10] O. Portillo Moreno, H. Lima Lima, R. Lozada Morales, R. Palomino Merino, O. Zelaya Ángel, Journal of Materials Science. **40** (2005) 1-4.

[11] L. P. Dishmukh, K. M. Garadakar, D. S. Strave, *Material Chemistry and Physics*, 55 (1998) 30-35.
[12] Mark Green and Paul O´Brien, Chem. Commun. (1999) 2235-2241.
[13] Gary Hodes, Phys. Chem. Chem. Phys. **9** (2007) 2181-2196.
[14] E. Pentia, L. Pintilie, Matei, T. Botila, E. Ozbay, Journal of Optoelectronics Material and Advanced Materials **3** (2001) 525-530.
[15] J. P. Yang, S. B. Quadri, and B. R. Ratna, J. Phys. Chem. **100** (1996) 17255-17259.
[16] Sushil Kumar, T. P. Sharma, M. Zulfequar, M. Husain, Physical **B 325** (2003) 8-16.
[17] Cardona M., Greenaway D. L. Phys Rev, **A 133** (1964) 1685-1690.
[18] Aspnes, D. E., Cardona, M. Phys. Rev, **173** (1968) 714-728.
[19] J. I. Contreras Rascón, O. Portillo Moreno, G. Abarca Ávila, J. R. Cerna, J. Hernández Tecorralco, J. Martinez Juárez, R. Lozada Morales and O. Zelaya Ángel, Journal of Materials Science and Engineering B1 (2011).
[20] Brajesh K, Rai, H. D. Bist, R. S. Katiyar M. T. S. Nair, P. K. Nair, A. Mannivannan, J. Appl. Phys. **82** (1997) 1310-1319.
[21] Rakesh K Joshi, and H. K. Sehgal, Structure, Nanotechnology **14** (2003) 592-596.
[22] Michael Kokotov and Gary Hodes, Chem. Mater. **22** (2010) 5483-5491.
[23] A. Rivera Márquez, M. Rubín Falfán, R. Lozada Morales, O. Portillo Moreno, O. Zelaya Ángel, J. Luyo Alvarado, M. Melendez Lira, L. Baños, phys. stat. sol. **188** (2001) 1059-1064.
[24] Bo Zhang, Guanghal Li, Jun Zhang, Young Zhang and Lide Zhang. Nanotechnology, **14** (2003) 443-44